Astron. Astrophys. 303, 223–232 (1995)

ASTRONOMY
AND
ASTROPHYSICS

Diffuse interstellar bands and UV extinction curves. The missing link*

F.-X. Désert[1,2], P. Jenniskens[3,2], and M. Dennefeld[4]

[1] Institut d'Astrophysique Spatiale, Bat 121, Université Paris XI, F-91405 Orsay Cedex, France (desert@ias.fr)
[2] Laboratory Astrophysics, Huygens Laboratorium, N. Bohrweg 2, Postbus 9504, 2300 RA Leiden, The Netherlands
[3] NASA/Ames Research Center, Mail Stop 239-4, Moffett Field, CA 94035-1000, USA (peter@max.arc.nasa.gov)
[4] Institut d'Astrophysique de Paris, 98bis Blvd Arago, F-75014 Paris, France (dennefeld@iap.fr)

Received 22 January 1993 / Accepted 27 February 1995

Abstract. The connection between diffuse interstellar bands and components of the interstellar ultraviolet extinction curve, decomposed according to the Fitzpatrick & Massa scheme, is analysed from new observations of several DIBs in the line of sight to 28 stars measured by IUE. We find that the strength of the 217.5 nm bump positively correlates with DIB strength, whereas correlations with a negative slope exist with the FUV non-linear rise and the width of the bump. There is no correlation with linear rise. The relation of bump height versus DIB strength does not pass through zero. The results are interpreted within the polycyclic aromatic hydrocarbon (PAH) framework. They strengthen the hypothesis that the FUV non-linear rise is produced by neutral PAHs, whereas DIB carriers are found among some ionised or radical PAHs.

Key words: dust, extinction – ISM: molecules – ISM: abundances

1. Introduction

Almost every article on diffuse interstellar bands (= *DIB*) starts by stating that, since the discovery that DIBs are interstellar (Merrill 1934), the nature of their carriers is still unknown. Unfortunately, this is true also for many other features of interstellar extinction. Notably, those components of the ultraviolet (= *UV*) extinction curve that are superposed on the gray extinction of large grains are not satisfactorily explained. On the other hand, most current hypotheses for the origin of the Diffuse Interstellar Bands allow for, or even imply, some connection with these extinction curve features. This can put important constraints on the carrier of DIBs if such a relationship can be established through observations (Wu 1972).

There have been two long-standing possible interpretations (or schools) for the origin of DIBs: one involves impurities in grains or grain mantles (e.g. Herbig 1975; Duley 1982; Shapiro & Holcomb 1986; Krelowski et al. 1987; Jura 1987) and the other invokes large molecules (e.g. Smith et al. 1977; Danks & Lambert 1976). In recent years, the latter school has gained favour because of a number of reasons: There is strong evidence for the existence of large molecules in the interstellar medium, tentatively identified as polycyclic aromatic hydrocarbons (= *PAH* - Léger & Puget 1984; Allamandola et al. 1985). Some emission bands in the Red Rectangle have now been associated with fluorescent emission of the DIB carriers (Sarre 1991; Fossey 1991). The DIB spectrum has become richer, amounting now to some 200 absorptions (Herbig & Leka 1991; Jenniskens & Désert 1994). And many of these DIBs are found to vary in strength with respect to each other. Such variations allow a grouping of DIBs in at least three DIB *families* with representative members λ4430 (λ6177), λ5780, and λ5797 respectively (Chlewicki et al. 1986; Krelowski & Walker 1987).

In both hypothesis one would expect some correlation between the DIBs and the UV extinction curve features that are superposed on the saturated big grain ($\simeq$ 0.1 μm) extinction. For example, small and very small grains have been invoked to account for the far UV rise (e.g. Hong & Greenberg 1980; Mathis & Whiffen 1989) and very small carbonaceous grains or PAHs are thought to cause the bump at 217.5 nm (e.g. Joblin et al. 1992). However, many studies (Wu 1972; Wu et al. 1981; Nandy et al. 1982; Witt et al. 1983; Seab & Snow 1984; Krelowski et al. 1987; Benvenuti & Porceddu 1989) have thus far given weak or negative results. We have examined these relationships from a homogeneous set of new DIB measurements of representative members of all three families (Sect. 2) and compared them to the shape parameters of the extinction curve introduced by Fitzpatrick & Massa (1986, 1988, 1990 - hereafter *FM*) rather than UV photometric colours (Sect. 3). We report in Sect. 4 that, indeed, some correlations are present. These results are compared

Send offprint requests to: F.-X. Désert [1] or P. Jenniskens [3]

* From observations obtained at the Observatoire de Haute-Provence, France

to previous finds and are discussed in the context of the PAH hypothesis (Sect. 5).

2. The DIB observations

Observations of Diffuse Interstellar Bands were carried out at the *Observatoire de Haute–Provence* (France) during two periods in Sept. 1990 and Sept. 1991. A total of 28 stars with a visual magnitude of +5 to +8 were observed. In addition, we will consider the 10 southern hemisphere stars from Benvenuti & Porceddu (1989) that are in common with the UV extinction curve sample of Aiello et al. (1988). This makes a total sample of 38 stars.

We maximised the number of observed DIBs per integration by choosing two spectral windows for each star centered at 5770 Å and 6240 Å respectively. The following DIBs were measured: Of the λ4430-family: λ6177; Of the λ5780-family: λ5705, λ5780, λ6269, and λ6284; And of the λ5797-family: λ5797 and λ5850. In addition, the narrow λ6196 was measured, which may be part of a fourth family (Jenniskens & Désert 1995).

Our northern hemisphere observations were done with a 1.52 m telescope and the AURELIE spectrograph (Gillet 1990). The 1200 groove/mm grating gives a spectral resolution of about 20,000 at the observed wavelengths. The detector is a Thomson reticon array of 2048 elements cooled to liquid nitrogen temperature and read by two CCDs. Three pixels correspond to one resolution element. Note that the large number of pixels allows a wide wavelength coverage, typically 200 Å in one integration. The relative response of each pixel is measured with an internal Tungstene lamp. Wavelength calibration is achieved with an internal Th–Ar lamp. These calibrations were done for each window and each observed star. Zero signal pixel values were measured as often as necessary. An OG 515 filter is used for the 6240 Å window to separate the dispersion orders. The stars were selected such as to be bright enough to give a good S/N and to represent the whole range of UV parameters in the sample. A signal to noise ratio per pixel of 100 could be achieved for a 7th magnitude star in typically less than 10 minutes of integration. Integration times were chosen in order to have a near constant noise level in the ratio of DIB equivalent width to E_{B-V}.

Reduction of the data was done with the IHAP processing package on HP computers (Observatoire de Haute–Provence and the Institut d'Astrophysique de Paris). The spectra were calibrated (see above) and corrected for cosmic rays. The baseline was taken to be of third order for the 5770 window and of second order for the 6240 window. The large spectral window allows a relative ease in placing the continuum on both sides of each DIB for the equivalent width measurements. Note that we both included the main peak and background features in Jenniskens & Désert (1994) for the bands λ6269, λ6284, and λ5705. The λ5780, however, does not include the broad λ5778, although this component was found to be part of the λ5780 profile in Jenniskens & Désert (1994). The high spectral resolution allowed an accurate removal of the atmospheric lines. The removal of the strong O_2 band near 6280 Å and the water features in the 5770 window was near perfect, with no remnant at a level of more than 2σ (Herbig 1975; Benvenuti & Porceddu 1989). The reference stars for atmospheric lines are η UMa and HD32630, both of type B3V with broad stellar lines. The stellar lines do not interfere with the DIB profiles. A sample of the spectra is given elsewhere (Jenniskens & Désert 1993, 1994), together with a discussion of new weak features superposed on the strongest DIBs.

3. The UV observations

In the present study, we will consider the large sample of 115 IUE extinction curves reduced by Aiello et al. (1988, hereafter *ABC*). The ABC sample mainly consists of line of sights that sample the diffuse medium, although some are clearly close to dense molecular clouds.

The extinction curve k(x) is conveniently expressed in terms of colour excess (E):

$$E_{\lambda-V} = (m_\lambda - m_V) - (m_\lambda - m_V)_o \quad (1)$$

These parameters refer to actually observed magnitudes at given wavelength and the index $)_o$ refers to the colour of an unreddened star of the same spectral type. The extinction curve in this representation is ($x = 1/\lambda$):

$$k(x) = E_{\lambda-V}/E_{B-V} \quad (2)$$

From a sample of 60 UV extinction curves observed with the *International Ultraviolet Explorer* (IUE), Fitzpatrick & Massa (1986, 1988) have shown that three distinct components are necessary to reproduce the UV extinction curve from $x = 3\ \mu\mathrm{m}^{-1}$ to $8\ \mu\mathrm{m}^{-1}$: 1) a linear increase throughout the UV ($c1 + c2 * x$); 2) a Drude profile characterising the so-called Bump at around 217.5 nm ($x_o = 4.5\ \mu\mathrm{m}^{-1}$); and, 3) a curvature term in the far UV (= *FUV*: $x \geq 5.9\ \mu\mathrm{m}^{-1}$):

$$k(x) = c1 + c2 * x + c3 * D(x, x_o, \gamma) + c4 * f(x) \quad (3)$$

The shape of the bump $D(x, x_o, \gamma)$ and the FUV non-linear rise $f(x)$ do not vary from one line of sight to another (Fitzpatrick & Massa 1986; Greenberg & Chlewicki 1983).

These components describe the degrees of freedom observed in a sample of extinction curves. Indeed, FUV non-linear rise, bump, and linear-rise vary independently, although extreme cases of bump height tend to anti–correlate with the FUV non-linear rise and strong bumps also tend to be a bit narrower (Fitzpatrick & Massa 1988; Jenniskens & Greenberg 1993).

The fitting procedure yields very good results. Hence, the relation of extinction and DIB absorption can be discussed independently of the interpretation of these mathematical components in terms of optical properties of astrophysically relevant materials. The true optical properties of the bump, for example, may contain a small fraction of the linear rise and FUV non-linear rise. Previous studies have concentrated on the bump

Table 1. Reddening and four FM parameters of the UV extinction curves of 38 ABC target lines of sight. Uncertainties are one sigma intervals

star	E(B-V)	+/-	C2	+/-	BH	+/-	Y	+/-	c4	+/-
HD 15558	0.75	0.04	0.65	0.05	4.32	0.31	0.94	0.03	0.49	0.06
HD 16691	0.83	0.07	0.70	0.07	4.22	0.40	0.95	0.03	0.47	0.06
HD 23060	0.34	0.01	0.22	0.09	3.81	0.48	1.06	0.06	0.44	0.11
HD 30614	0.32	0.05	0.85	0.16	3.44	0.73	0.94	0.07	0.14	0.12
HD 34078	0.52	0.06	0.57	0.09	3.51	0.51	1.09	0.04	0.52	0.09
HD 36879	0.50	0.06	0.62	0.10	4.14	0.59	0.76	0.04	0.28	0.08
HD 37367	0.43	0.06	0.49	0.10	4.54	0.73	0.94	0.05	0.30	0.10
HD 37903	0.38	0.06	0.34	0.10	2.68	0.60	1.13	0.06	0.50	0.13
HD 38131	0.51	0.06	0.78	0.11	4.42	0.61	0.95	0.04	0.37	0.08
HD 154445	0.43	0.07	0.23	0.08	4.32	0.80	1.05	0.05	0.50	0.12
HD 166937	0.51	0.05	0.03	0.06	1.96	0.37	0.95	0.04	0.30	0.08
HD 168076	0.80	0.06	0.48	0.05	3.33	0.32	0.93	0.03	0.46	0.06
HD 168112	1.04	0.09	0.49	0.05	3.93	0.37	0.86	0.02	0.36	0.05
HD 183143	1.24	0.08	0.31	0.03	4.36	0.31	0.93	0.02	0.42	0.04
HD 190603	0.94	0.02	0.67	0.03	2.58	0.18	0.92	0.02	0.03	0.04
HD 192281	0.73	0.07	0.74	0.08	3.68	0.42	0.95	0.03	0.42	0.06
HD 193682	0.83	0.06	0.71	0.06	4.51	0.38	1.05	0.03	0.19	0.05
HD 199216	0.73	0.01	0.67	0.04	3.87	0.23	1.03	0.03	0.51	0.05
HD 199579	0.38	0.05	0.65	0.12	2.94	0.57	1.12	0.06	0.69	0.13
HD 209339	0.37	0.01	0.74	0.08	4.09	0.45	1.02	0.06	0.23	0.10
HD 216532	0.87	0.08	0.53	0.06	3.80	0.39	1.08	0.02	0.39	0.06
HD 216898	0.88	0.09	0.51	0.06	3.91	0.44	0.98	0.02	0.36	0.06
HD 217086	0.92	0.05	0.51	0.04	4.23	0.29	1.01	0.02	0.38	0.05
HD 239729	0.67	0.01	0.64	0.05	2.99	0.24	1.13	0.03	0.76	0.06
HD 242908	0.62	0.03	0.52	0.05	3.55	0.31	0.90	0.03	0.44	0.06
BD+31 643	0.85	0.03	0.51	0.04	3.28	0.22	1.28	0.02	0.58	0.05
BD+60 497	0.89	0.06	0.59	0.05	3.85	0.32	0.98	0.02	0.72	0.06
BD+63 1964	0.95	0.02	0.73	0.04	3.96	0.19	0.91	0.02	0.46	0.04
HD 303308	0.46	0.06	0.55	0.10	3.33	0.56	0.94	0.05	0.43	0.10
HD 122879	0.37	0.06	0.55	0.12	4.14	0.80	1.00	0.06	0.32	0.11
HD 123008	0.63	0.03	0.68	0.06	3.58	0.31	0.88	0.03	0.22	0.06
HD 152233	0.45	0.06	0.74	0.12	3.70	0.61	1.00	0.05	0.45	0.10
HD 152247	0.44	0.06	0.81	0.13	3.91	0.65	0.95	0.05	0.47	0.11
HD 152248	0.45	0.06	0.74	0.12	3.63	0.60	0.93	0.05	0.35	0.09
HD 152249	0.46	0.06	0.74	0.12	3.83	0.61	1.02	0.05	0.26	0.09
HD 162978	0.38	0.06	0.51	0.11	3.31	0.67	0.95	0.06	0.16	0.10
HD 164794	0.36	0.03	0.34	0.09	3.73	0.54	0.99	0.06	0.41	0.11
HD 165052	0.46	0.06	0.37	0.08	3.56	0.58	0.96	0.05	0.26	0.09

height (= *BH*), which is equal to c_3/γ^2 in the FM parametrisation, and on the *FUV rise*, which is a combination of the linear rise (c_2) and the far UV non-linear rise (c_4).

The FM decomposition procedure was applied to the ABC sample by Jenniskens & Greenberg (1992) and the resulting UV parameters for our sample of stars are given in Table 1. These values are in units of k(x), hence, normalised to reddening E_{B-V}. They will be compared to the integrated band strength (equivalent width) of eight DIBs, normalized to E_{B-V} in a similar way as the extinction curve parameters. The values for E_{B-V} quoted by ABC were compared to those derived from new photometric measurements in the Hipparcos input catalogue (1992). Only one significant difference occurs: E_{B-V} of the star HD 166937 is a factor of two higher.

4. Results

4.1. The DIB–UV correlation analysis

Throughout this paper, we will consider the *DIB strength*, defined as the equivalent width normalised to reddening: W/E_{B-V}. It measures the relative amount (i.e. the abundance

Table 2a. Equivalent width normalised to unit redding E_{B-V} of the strongest DIBs observed in the 5770 Å window (Table 2a) and 6240 Å window (Table 2b). Units are: Å mag^{-1}. Data of the series starting at HD303308 until HD165052 are from Benvenuti & Porceddu (1989)

star	5707	+/-	5780	+/-	5797	+/-	5850	+/-
HD15558	0.195	0.011	0.603	0.032	0.172	0.010	0.068	0.005
HD16691	0.222	0.020	0.342	0.030	0.077	0.008	0.035	0.007
HD23060	0.103	0.004	0.350	0.011	0.144	0.005	0.032	0.003
HD30614	0.050	0.008	0.347	0.054	0.141	0.022	0.056	0.009
HD34078	0.117	0.014	0.265	0.031	0.083	0.010	0.038	0.005
HD36879	0.190	0.023	0.582	0.070	0.106	0.013	0.064	0.008
HD37367	0.305	0.043	0.970	0.135	0.198	0.028	0.088	0.013
HD37903	0.182	0.029	0.384	0.061	0.145	0.023	0.008	0.005
HD38131	0.255	0.030	0.757	0.089	0.167	0.020	0.061	0.008
HD154445	0.172	0.028	0.381	0.062	0.123	0.020	0.026	0.006
HD166937	0.153	0.015	0.476	0.047	0.137	0.014	0.047	0.006
HD168076	0.122	0.012	0.465	0.036	0.209	0.016	0.054	0.009
HD168112	0.121	0.014	0.419	0.037	0.108	0.011	0.054	0.010
HD183143	0.156	0.012	0.581	0.038	0.144	0.010	0.055	0.007
HD190603	0.101	0.004	0.347	0.008	0.074	0.003	0.027	0.003
HD192281	0.092	0.009	0.368	0.035	0.141	0.014	0.055	0.006
HD193682	0.149	0.012	0.453	0.033	0.088	0.007	0.043	0.005
HD199216	0.070	0.005	0.255	0.006	0.133	0.003	0.064	0.005
HD199579	0.124	0.017	0.276	0.036	0.111	0.015	0.045	0.006
HD209339	0.214	0.006	0.597	0.016	0.168	0.005	0.076	0.003
HD216532	0.161	0.015	0.495	0.046	0.137	0.013	0.057	0.006
HD216898	0.153	0.016	0.500	0.051	0.160	0.017	0.073	0.008
HD217086	0.155	0.009	0.538	0.029	0.157	0.009	0.058	0.005
HD239729	0.087	0.003	0.279	0.005	0.110	0.003	0.046	0.003
HD242908	0.182	0.011	0.574	0.029	0.077	0.006	0.042	0.007
BD+31 643	0.134	0.006	0.305	0.011	0.092	0.004	0.047	0.004
BD+60 497	0.143	0.011	0.444	0.030	0.137	0.010	0.079	0.008
BD+63 1964	0.145	0.006	0.683	0.015	0.236	0.006	0.104	0.006
HD303308	-.---	-.---	0.574	0.075	0.124	0.016	-.---	-.---
HD122879	-.---	-.---	0.841	0.136	0.203	0.033	-.---	-.---
HD123008	-.---	-.---	0.787	0.037	0.202	0.010	-.---	-.---
HD152233	-.---	-.---	0.353	0.047	0.187	0.025	-.---	-.---
HD152247	-.---	-.---	0.509	0.069	0.180	0.025	-.---	-.---
HD152248	-.---	-.---	0.507	0.068	-.---	-.---	-.---	-.---
HD152249	-.---	-.---	0.559	0.073	0.148	0.019	-.---	-.---
HD162978	-.---	-.---	0.550	0.087	0.158	0.025	-.---	-.---
HD164794	-.---	-.---	0.447	0.037	0.094	0.008	-.---	-.---
HD165052	-.---	-.---	0.459	0.060	0.122	0.016	-.---	-.---

average) of the DIB carriers along each line of sight (Tables 2 and 3).

Figures 1 show the relationship between DIB strength (vertical axis) and UV extinction (horizontal axis). The UV extinction parameters are described in Sect. 2. Figure 1a gives correlation diagrams for some of the narrow DIBs of the λ5797 and λ6169 families. Correlation coefficients are given in Table 3. The full-width-at-half-maximum (FWHM) of these bands is 0.44, 0.84, and 0.91 Å for λ6196, λ5797, and λ5850 respectively (Jenniskens & Désert 1994, after correction for instrumental broadening). Figure 1b shows similar data for three broader DIBs of the λ5780 and λ4430 families. The full width at half maximum of λ6269, λ5780, and λ6177 is 2.50, 2.01, and 23.0 Å respectively. Only part of the program stars give useful information on λ6177 because of stellar line contamination and flatfielding imperfections.

The following results can be drawn from the present data set:

* No correlation is seen between the normalised strength of DIBs and the linear rise in the UV (c_2).

Table 2b.

star	6195	+/-	6177	+/-	6269	+/-	6284	+/-
HD15558	0.059	0.004	0.875	0.048	0.183	0.010	1.876	0.100
HD16691	-.---	-.---	-.---	-.---	-.---	-.---	-.---	-.---
HD23060	-.---	-.---	-.---	-.---	-.---	-.---	-.---	-.---
HD30614	0.050	0.008	0.472	0.075	0.197	0.031	1.169	0.183
HD34078	0.040	0.050	0.385	0.045	0.110	0.013	1.244	0.144
HD36879	0.058	0.007	0.690	0.083	0.146	0.018	1.924	0.231
HD37367	0.105	0.015	1.284	0.179	0.249	0.035	2.416	0.337
HD37903	0.042	0.007	0.579	0.092	0.087	0.014	1.089	0.172
HD38131	0.090	0.011	-.---	-.---	0.271	0.032	2.188	0.249
HD154445	0.040	0.007	0.442	0.073	0.177	0.029	1.067	0.174
HD166937	0.043	0.004	0.614	0.060	0.073	0.007	1.669	0.164
HD168076	0.049	0.004	-.---	-.---	0.155	0.012	1.389	0.104
HD168112	0.043	0.006	0.524	0.049	0.113	0.011	1.284	0.111
HD183143	0.077	0.006	-.---	-.---	0.170	0.011	1.508	0.097
HD190603	0.034	0.001	0.437	0.010	0.065	0.002	1.352	0.029
HD192281	0.045	0.004	0.312	0.030	0.100	0.010	1.059	0.102
HD193682	0.071	0.005	-.---	-.---	0.159	0.012	0.276	0.020
HD199216	0.032	0.004	0.363	0.017	0.092	0.005	0.786	0.013
HD199579	0.032	0.005	0.318	0.043	0.111	0.015	0.724	0.095
HD209339	0.068	0.002	0.786	0.022	0.189	0.005	1.927	0.052
HD216532	0.045	0.004	0.595	0.055	0.171	0.016	1.448	0.133
HD216898	0.068	0.007	0.639	0.066	0.128	0.013	1.390	0.142
HD217086	0.053	0.004	0.564	0.032	0.143	0.008	1.368	0.074
HD239729	0.048	0.002	-.---	-.---	0.125	0.003	0.587	0.009
HD242908	-.---	-.---	-.---	-.---	-.---	-.---	1.661	0.081
BD+31 643	0.041	0.013	0.232	0.054	0.062	0.015	0.878	0.040
BD+60 497	0.065	0.006	-.---	-.---	0.191	0.014	1.188	0.080
BD+63 1964	0.060	0.006	0.828	0.031	0.171	0.008	1.616	0.036
HD303308	0.048	0.007	-.---	-.---	0.217	0.029	1.272	0.166
HD122879	0.068	0.011	-.---	-.---	0.214	0.035	1.816	0.294
HD123008	0.075	0.004	-.---	-.---	0.183	0.009	1.933	0.092
HD152233	0.053	0.007	-.---	-.---	0.131	0.017	0.993	0.132
HD152247	0.048	0.007	-.---	-.---	0.123	0.017	0.811	0.111
HD152248	0.049	0.007	-.---	-.---	0.111	0.015	0.856	0.114
HD152249	0.048	0.006	-.---	-.---	0.107	0.014	1.139	0.149
HD162978	0.055	0.009	-.---	-.---	0.111	0.018	1.050	0.166
HD164794	0.047	0.004	-.---	-.---	0.114	0.009	0.978	0.081
HD165052	0.043	0.006	-.---	-.---	0.174	0.023	1.009	0.132

* There is a trend for the DIB strength to correlate with the bump height BH = c_3/γ^2. The intercept of this correlation does not go through zero. Strong changes in DIB strength correspond to only weak variations of bump strength.

* There is a trend for DIB strength to anti-correlate with the bump width γ.

* There is a similar trend for DIB strength to anti–correlate with the FUV non-linear rise. Notable exceptions are HD190603 and HD30614 which have lowest c_4.

* All DIB families show a similar behavior except, perhaps, that the anti-correlation with FUV non-linear rise is stronger for the λ5780 and λ4430 families.

A "weak" correlation refers to scatter significantly larger than the measurement error. Correlations with λ5797 are least convincing, but these may be affected by larger uncertainties than accounted for due to contamination by [*C*IV] stellar lines in O–type stars. Most other correlations are limited by the uncertainties in the normalised UV parameters, not those in the DIB measurements.

Table 3. Correlation coefficients for the relations of normalised DIB strength W/E_{B-V} versus the extinction curve parameters, before (r) and after (r_c) correction for observational errors (Jenniskens & Greenberg 1993). These values were calculated after omitting the two most extreme points: linear rise c_2 without HD166937 and HD30614, bump height BH without HD166937 and HD37367, bump width γ without HD63879 and BD+31 643, and FUV non-linear rise without HD30614 and HD190603

W/E_{B-V}	r:				r_c:			
	c_2	BH	γ	c_4	c_2	BH	γ	c_4
λ6196	+0.10	+0.60	-0.31	-0.38	+0.12	+0.99	-0.41	-0.48
λ5797	+0.16	+0.21	-0.24	-0.23	+0.19	+0.35	-0.30	-0.27
λ5850	+0.41	+0.43	-0.41	-0.18	+0.48	+0.71	-0.51	-0.21
λ6269	-0.01	+0.53	-0.21	-0.19	-0.01	+0.91	-0.27	-0.23
λ5707	+0.05	+0.49	-0.16	-0.43	+0.06	+0.83	-0.20	-0.52
λ5780	+0.10	+0.43	-0.45	-0.56	+0.12	+0.73	-0.57	-0.67
λ6284	-0.00	+0.32	-0.44	-0.34	-0.00	+0.54	-0.56	-0.41
λ6177	+0.02	+0.49	-0.33	-0.59	+0.02	+0.82	-0.41	-0.70
average:	+0.10	+0.44	-0.32	-0.36	+0.12	+0.74	-0.40	-0.44
median:	+0.07	+0.46	-0.32	-0.36	+0.09	+0.78	-0.41	-0.45

4.2. E_{B-V} dependence

It is difficult to see how a systematic bias could produce the results above. DIB strength and UV extinction curve parameters are measured from independent techniques and by independent observers. Both refer to extinction measurements and the same line of sight is sampled.

The random uncertainty in the common parameter E_{B-V} do not produce the correlations. Figure 2 shows correlation diagrams of DIB strength versus reddening. To guide the eye, DIB strength is now normalised by the constant "diffuse medium" value of W/E_{B-V} listed by Jenniskens & Désert (1994). A dashed line indicates the slope of an E_{B-V}^{-1} dependence in this log-log plot. Indeed, there is no correlation of DIB strength with E_{B-V}. As expected, the DIB abundance does not correlate with column density of all matter in the line of sight.

Note the slight negative trends in the lower three plots of Fig. 2 (λ5780 and λ4430 families) as opposed to those in the upper plots (λ6196 and λ5797 families). This is the family behavior reported by Jenniskens et al. (1994) due to the sensitivity of DIB strength to location inside a dense molecular cloud (Snow & Cohen 1974). The weakening of DIB strength inside a molecular cloud is stronger per unit extinction for the λ4430 and λ5780 families than for the λ6196 and λ5797 families. The effect is less obvious here because most of the lines of sight in the ABC sample refer to the (low density) diffuse medium.

5. Discussion

5.1. Comparison with previous related studies

Over the years, there has been a steady stream of publications dedicated to finding relationships between UV extinction and DIB absorption. Weak trends and outright negative results have been reported, but only now has it become clear which part of the extinction curve relates to DIB strength behaviour.

Early studies only considered DIB absorption and UV extinction curve colours before normalisation to unit reddening (or unit extinction in the visual). Wu (1972) used OAO-2 extinction measurements at 2175, 3500, and 1200 Å in combination with high resolution (0.23 Å) echelle spectra of DIBs λ4430, λ5780, and λ5797 in 66 lines of sight. By using $E_{2175-3500}$ as a measure of bump strength and E_{1200-V} as a measure of rise in the extinction curve, Wu found that λ5780 and λ5797 correlated better with E_{B-V} than with $E_{2175-3500}$ and that there was no correlation with E_{1200-V}. Wu (1972) found a hint that correlations involving λ4430 were worse than those of the other DIBs, suggesting family behavior, but this was subsequently proven to merely reflect larger uncertainties in the λ4430 data (Nandy & Thompson 1975; Dorschner et al. 1977; Wu et al. 1981).

Herbig (1975) noticed that the correlation of DIB strength with colours becomes worse when colours are considered above the turning point in the extinction curve; that is where the linear rise starts to contribute significantly to the total extinction (Jenniskens 1994). Wu et al. (1981) confirmed that the correlation of λ4430 with extinction at 2500 Å and shorter wavelengths is progressively weaker.

Witt et al. (1983) were the first to consider the relative band strength. They compared 20 IUE extinction curves with DIB measurements in Snow et al. (1977). The parameters k(2175), k(2160), and k(1250) are proportional to the bump, the linear rise, and a sum of linear rise plus FUV non-linear rise, respectively. They found a weak positive correlation of A_c4430/E_{B-V} with normalised bump strength, in good agreement with our data. A weak negative correlation was found with the sum of linear and non-linear rise at 1250 Å. We now attribute this negative trend to an anti-correlation with the FUV non-linear rise.

Seab & Snow (1984) normalised IUE data of 50 stars to E_{B-V} and also found a weak positive correlation between the depth of the 4430 band and the normalised bump strength. No other correlations were found. Their normalisation procedure, however, considered an excess from a linear fit through the general depth versus reddening relationship which has a non-zero intercept. Such non-zero intercept is now thought to be mainly the result of observational errors in the list compiled by Snow et al. (Somerville 1988).

Until the mid eighties, the limitation of correlation studies was thought to be the accuracy of the DIB measurements and not the accuracy of the UV extinction curves (Wu et al. 1981). In 1987, Krelowski et al. (1987) considered Reticon observations of λ4430, while the first CCD observations of 37 stars with known IUE extinction curves were performed by Josafatsson & Snow (1987). Josafatsson & Snow found that the equivalent

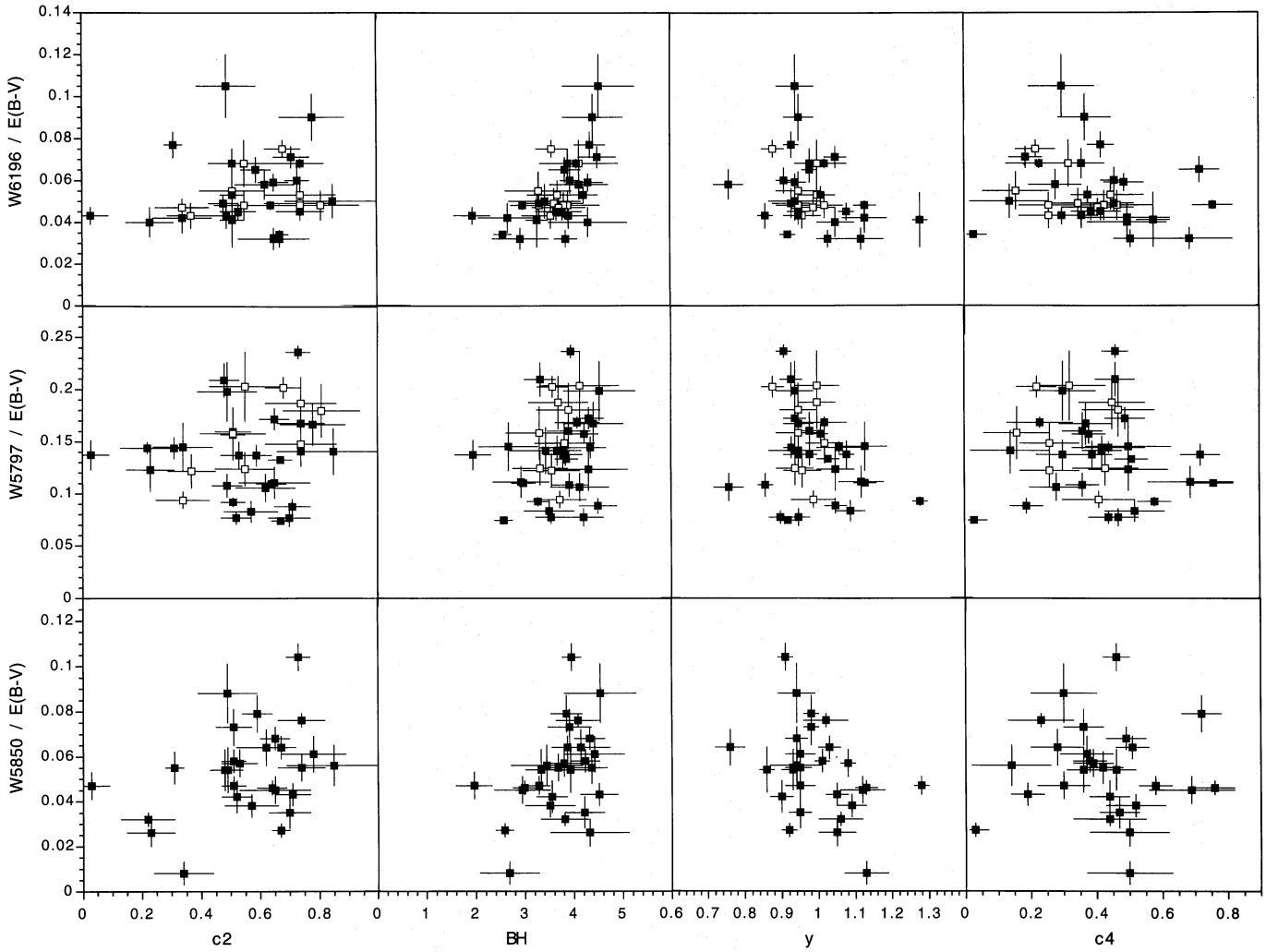

Fig. 1a. Correlation diagrams for three narrow DIBs λ6196, λ5797, and λ5850 (Fig. 1a) and three broader DIBs λ6269, λ5780, and λ6177 (Fig. 1b). Rows give the normalised equivalent width W/E_{B-V}. Columns give the correlation with linear rise, bump height, bump width, and FUV non-linear rise respectively. Open symbols are data by Benvenuti & Porceddu (1989)

width of the broad 5778 correlates well with the bump strength, while other bands showed no significant correlation. This result was stained by small sample size (N=6 to 14). The FUV extincton was considered by Krelowski et al. (1987), who compared excess absorption (including a non-zero intercept) of λ4430 to ANS extinction data. They found again an anti-correlation with $E_{1500-1800}$, but only for a combination of lines of sight to the Per OB1 and Cep OB3 associations. This ANS colour excess relates to the FUV non-linear rise, but is also sensitive to CIV stellar line contamination and contains a significant component of the linear rise. Indeed, the correlation disappeared when stars of other associations at higher latitude were added. We now believe this was because of adding lines of sight with deviating linear rise.

Benvenuti & Porceddu (1989) first pursued the possible family dependence of the correlation of DIBs with the bump by correlating λ5780, λ5797, λ6196, λ6203, λ6270, and λ6284 of 26 Southern hemisphere stars with IUE UV extinction curves. Principal component analysis was applied to the dataset after normalising to unit reddening. The first eigenvalue was found at 55% confidence level and five variables were needed to increase this value to 93%. These values reflect the family behavior, because no significant differences were found among the families' relation to bump strength, which is confirmed here.

We conclude that previous studies, although reporting weak or negative results, are in agreement with the weak trends reported here. In addition, the FM parametrisation has helped us in finding other relevant UV parameters for DIB correlation studies, notably by making a distinction between linear rise and FUV non-linear rise and by considering the bump width.

5.2. *Implications*

From an observational point of view, these correlations were found to be useful for finding lines of sight with strong DIBs from a sample of UV extinction curves. The results are difficult to interpret theoretically, however, because the origin of both the

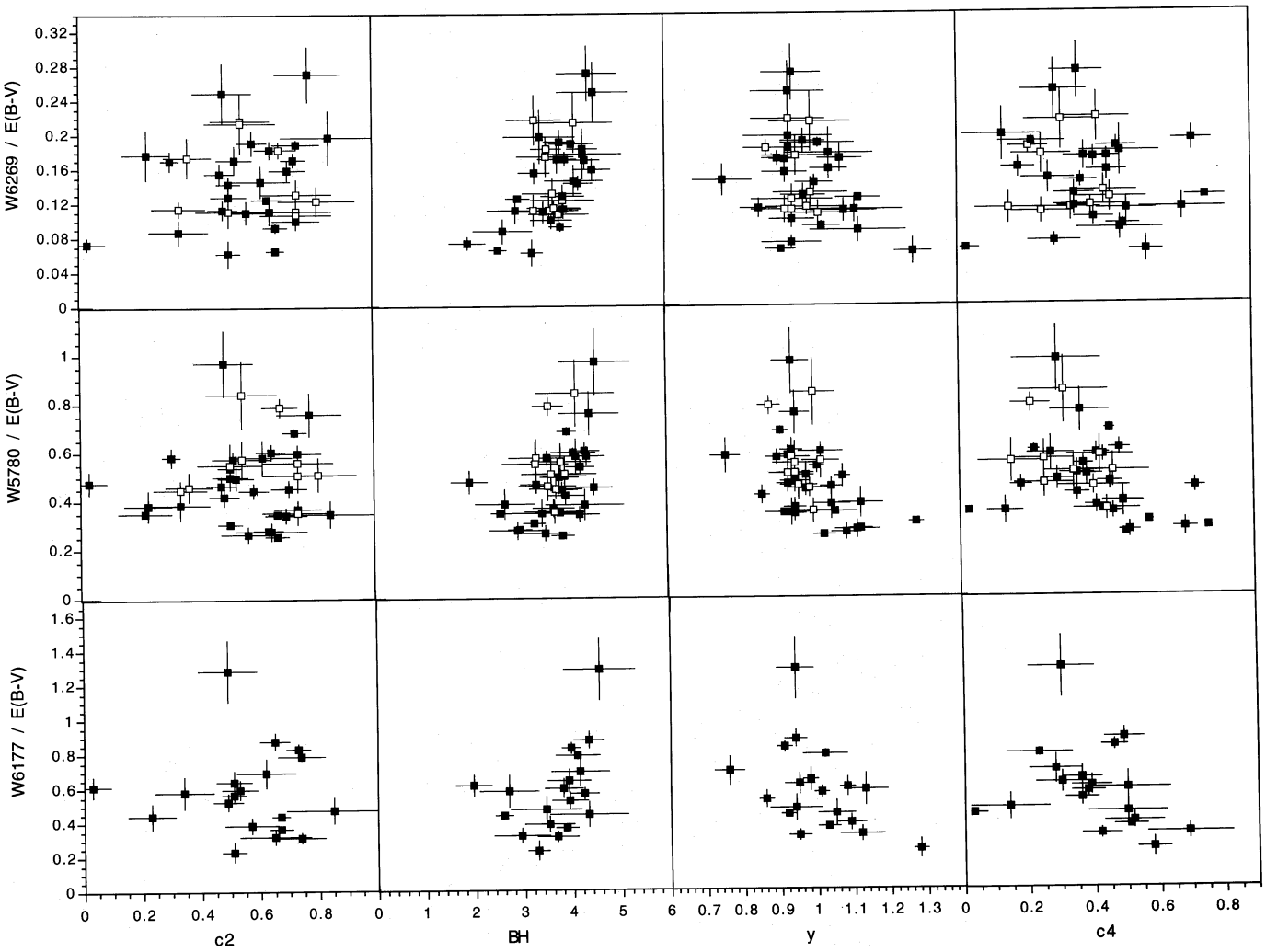

Fig. 1b.

UV extinction curve features and the DIB carriers is not well understood.

These correlations reflect the known loose relationships between bump height, bump width, and the FUV non-linear rise (Fitzpatrick & Massa 1988; Jenniskens & Greenberg 1993). It is possible that a single environmental parameter underlays the weak correlations of Fig. 1. The question is which parameter that could be.

The weak correlation with bump height suggests some proportionality in abundances. The bump is a pure absorption feature in most lines of sight and is generally not saturated. A linear least squares fit in a diagram of DIB strength versus bump strength does not go through zero, which implies that bump carrier and DIB carrier are not strictly the same. In fact, small variations in bump strength are associated with large variations in DIB strength. Whatever affects DIBs has much less effect on bump strength.

Perhaps an answer can be found in the anti-correlation with FUV non-linear rise. This FUV non–linear rise was found to correlate well with the abundance of CH, or neutral hydrogen for that matter (Jenniskens et al. 1992). A strong FUV non-linear rise corresponds to an environment rich in molecular hydrogen. DIB carriers apparently avoid such an environment. Indeed, the anti-correlation with FUV non-linear rise is strongest for DIBs that weaken most strongly in dense molecular clouds where hydrogen is in molecular form, i.e. the λ5780 and λ4430 families (Snow & Cohen 1974; Jenniskens et al. 1994).

The decrease of DIB strength is not related to the accretion of small grains on large grains in dense clouds. The DIB strength does not correlate with the linear rise in the extinction curve, which is related to the selective extinction $R_V = A_V/E_{B-V}$ (Cardelli et al. 1988, 1989). The decrease of linear rise in dense cloud environments is thought to reflect the accretion of small grains on larger grains.

DIB strength may, instead, be affected by the attenuation of the UV field inside dense clouds, which affect the ionisation state or dehydrogenation state of large molecules. Indeed, the behaviour of DIB strength in media of different hydrogen states (H^+,H,H_2) was previously found to be consistent with a molecular carrier in a singly (positively) ionised state (Jenniskens et al. 1994).

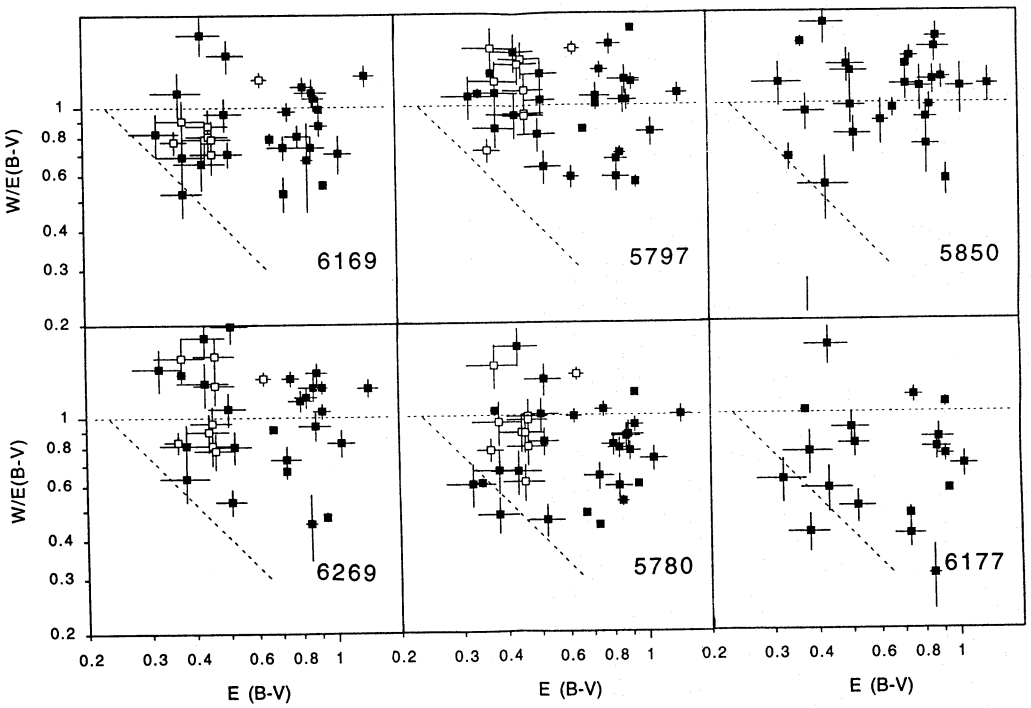

Fig. 2. The DIB strength W/E_{B-V} is plotted as a function of reddening. The slight negative trends in the lower three plots (λ4430 and λ5780 families) as opposed to those in the upper plots (λ6196 and λ5797 families) are discussed in the main text

5.3. Candidate carriers

There is strong evidence for the existence of large molecules that can survive in the diffuse interstellar (IS) medium. They are known through their very characteristic infrared (IR) emission features mainly at 3.3, 6.2, 7.7, 8.6 and 11.3 μm (Sellgren 1981). Léger & Puget (1984) and Allamandola et al. (1985) have interpreted these emission features as produced by polycyclic aromatic hydrocarbon (PAH) molecules that are large enough (at least 20 carbon atoms) to withstand the absorption of UV photons. Ionised PAHs have strong absorptions in the visual and near infrared, which led Crawford et al. (1985), Léger & d'Hendecourt (1985) and van der Zwet & Allamandola (1985), followed by Chlewicki et al. (1987), to consider ionised PAHs as possible candidates for DIBs.

Within the framework of the PAH hypothesis, we propose the following tentative explanation. The FUV non-linear rise may reflect the neutral fraction of the PAHs (see optical constants in Verstraete & Léger 1992). Ionised PAHs are expected to have a less strong FUV non-linear rise, because all energy states are shifted to higher energy (Jenniskens et al. 1992). Small ionised PAHs (of size less than about 60 carbon atoms) are known to have strong transitions in the visible whereas neutral PAHs do not. If DIBs are due to some *ionised* PAH species, then a low degree of PAH ionisation will result in relatively weak DIBs and a large FUV non–linear rise.

We note that in the PAH hypothesis (Léger & d'Hendecourt 1985), the DIB carriers need only to be a small fraction (0.1% to 1% depending on the oscillator strength) of the total PAH abundance which is about 10% of the available cosmic carbon. Hence, in this scenario bump strength and FUV non-linear rise can behave independently only when the bump contains a significant fraction of very small (carbonaceous) grains that do not contribute to the FUV non-linear rise (e.g. Joblin et al. 1992, and see the optical constants of Henrard et al. 1993).

The notable exceptions from the general correlation in Fig. 1 involving the FUV non-linear rise c_4 (HD 190603 and HD 30614) may indicate lower than average PAH abundances but a larger fraction of matter being ionized. These are IRAS infrared point sources where dust is found close to a hot star. Intense UV irradiation fields have been correlated with weak PAH signatures suggesting that PAHs are destroyed in HII regions (Boulanger et al. 1988; Jenniskens & Désert 1993a).

Alternatively, the variations may be related to hydrogenation of PAHs or small carbonaceous grains, where both DIB strength and bump strength reflect the strength of the local UV radiation field. Such phenomena have been invoked to explain the weak correlations found among the UV extinction curve parameters.

The results are more difficult to interpret in the light of the small MgO grain model for the bump suggested by MacLean et al. (1982), where impurities in the grains may broaden the bump. Such impurities are thought also to be responsible for the DIBs (Duley 1979), hence we should observe a correlation and not an anti–correlation between bump width and DIB strength. Furthermore, Herbig & Leka (1991) showed that several expected transitions of Cr^{3+}:MgO are not present in the DIB spectrum. The DIB strength does not reflect the abundance of free small grains, proportional to the strength of the linear rise (or R_V). When the small grains accrete on big grains, the DIB absorption is expected to be attenuated and changed in position and shape.

Changes in position and shape have not been reported thusfar, and we do not find an attenuation of the DIB carrier.

In conclusion, the weak correlation with bump strength and the anti-correlations with bump width and FUV non-linear rise found in this paper strengthen the big molecule hypothesis and argue against impurity sites in small grains.

Acknowledgements. We wish to thank the staff of OHP for their support during the observations, F. Barsella for having provided the digitised extinction curves of the ABC sample of stars, and P. Boissé and G. Chlewicki for helpful discussions. F.–X. D. acknowledges an European Space Agency external fellowship. Part of this work was done while at Laboratory Astrophysics in Leiden.

References

Aiello S., Barsella B., Chlewicki G. et al., 1988, A&AS 73, 195 (ABC)
Allamandola L.J., Tielens A.G.G.M., Barker J.R., 1985, ApJ 290, L25
Benvenuti P., Porceddu I., 1989, A&A 223, 329
Boulanger F., Beichman C., Désert F.-X. et al., 1988, ApJ 332, 328
Cardelli J.A., Clayton G.C., Mathis J.S., 1988, ApJ 329, L33
Cardelli J.A., Clayton G.C., Mathis J.S., 1989, ApJ 345, 245
Chlewicki G., van der Zwet G.P., van IJzendoorn L.J. et al., 1986, ApJ 305, 455
Chlewicki G., de Groot M.S., van der Zwet G.P. et al., 1987, A&A 173, 131
Crawford M.K., Tielens A.G.G.M., Allamandola L.J., 1985, *ApJL* 293, L45
Danks A. C., Lambert D. L., 1976, MNRAS 174, 571
Dorschner J., Friedemann C., Gurtler J., 1977, A&A 58, 201
Duley W.W., 1979, ApJ 227, 824
Duley W.W., 1982, ApSS 88, 501
Fitzpatrick E.L., Massa D., 1986, ApJ 307, 286
Fitzpatrick E.L., Massa D., 1988, ApJ 328, 734
Fitzpatrick E.L., Massa D., 1990, ApJS 72, 163 (FM)
Fossey S.J., 1991, Nature 353, 393.
Gillet D., 1990, OHP Aurelie Users' Manual.
Greenberg J.M., Chlewicki G., 1983, ApJ 272, 563
Henrard L., Lucas A.A., Lambin Ph., 1993, ApJ 406, 92
Herbig G. H., 1975, ApJ 196, 129
Herbig G. H., Leka K.D., 1991, ApJ 382, 193
Hipparcos Input catalogue, 1992, ESA publication SP–1136
Hong S.S., Greenberg J.M., 1980, A& A 88, 194
Jenniskens P., 1994, A&A 284, 227
Jenniskens P., Ehrenfreund P., Désert F.–X., 1992, A&A, 265, L1
Jenniskens P., Greenberg J.M., 1993, A&A 274, 439
Jenniskens P., Désert F.–X., 1993, A&A 274, 465
Jenniskens P., Désert F.–X., 1993a, A&A 275, 549
Jenniskens P., Désert F.–X., 1994, A&AS 106, 39
Jenniskens P., Désert F.–X., 1995, in *The Diffuse Interstellar Bands*, ed. A.G.G.M. Tielens, T.P. Snow, Kluwer Acad. Publ., in press.
Jenniskens P., Ehrenfreund P., Foing B., 1994, A&A 281, 517
Joblin C., Léger A., Martin P., 1992, ApJ 393, L79
Josafatsson K., Snow T.P., 1987, ApJ 319, 436
Jura M., 1987, in *PAHs and Astrophysics*, ed. A. Léger, L. d'Hendecourt, and N. Boccara (Kluwer: Dordrecht), p. 367
Krelowski J., Walker G.A.H., 1987, ApJ 312, 860
Krelowski J., Walker G.A.H., Grieve G.R., Hill G.M., 1987, ApJ 316, 449
Léger A., Puget J.–L., 1984, A&A 137, L5
Léger A., d'Hendecourt L., 1985, A&A 146, 81
MacLean S., Duley W.W., Millar T.J., 1982, ApJ 256, L61
Mathis J.S., Whiffen G., 1989, ApJ 341, 808
Merrill P. W., 1934, PASP 46, 206
Nandy K., Thompson G.I., 1975, MNRAS 173, 237
Nandy K., Morgan D. H., Houziaux L., 1982, ApJS 85, 159
Sarre P.J., 1991, Nature 351, 356
Seab C.G., Snow T.P., 1984, ApJ 277, 200
Sellgren K., 1981, ApJ 245, 138
Shapiro P.R., Holcomb K.A., 1986, ApJ 310, 872
Smith W.H., Snow T.P., York, D. G., 1977, ApJ 218, 124
Snow T.P., Cohen J.G., 1974, ApJ 194, 313
Snow T.P., York D.G., Welty D.E., 1977, AJ 82, 113
Somerville W.B., 1988, in *Interstellar Dust: Contributed Papers*, NASA Conf. Publ. 3036, Tielens & Allamandola eds., p. 77
van der Zwet G.P., Allamandola L.J., 1985, A&A 146, 76
Verstraete L., Léger A., 1992, A&A 266, 513
Witt A.N., Bohlin R.C., Stecher T.P., 1983, ApJ 267, L47
Wu C.-C., 1972, ApJ 178, 681
Wu C.-C., York D.G., Snow T.P., 1981, AJ 86, 755

This article was processed by the author using Springer-Verlag TEX A&A macro package 1992.